An Experimental Investigation of Sensitivity Dependence with respect to Waveguide Position on a Micromachined Diaphragm in a Silicon-Based Integrated Optic Pressure Sensor

Takeshi Goto[a], Atsushi Yamada[a], Masashi Ohkawa[*b], Seishi Sekine[b], and Takashi Sato[b]

[a]Niigata University, Graduate School of Science and Technology, Ohkawa Lab.
8050 Ikarashi 2-no-cho, Niigata 950-2181, Japan
[b]Niigata University, Faculty of Engineering
8050 Ikarashi 2-no-cho, Niigata 950-2181, Japan

ABSTRACT

We have been developing a silicon-based integrated optic pressure sensor using an intermodal interference between the fundamental TM-like and TE-like modes. The sensor has a micromachined diaphragm with a sensing waveguide as a pressure-sensitive structure. The sensor is theoretically known to have a strong dependence of sensitivity on the sensing waveguide on the diaphragm. According to the theoretical prediction for the sensor based on the elasto-optic effect, the waveguide should be placed along the diaphragm edge to maximize sensitivity. To date, such dependence has not been experimentally examined in detail. In this study, two sensors with 20 or more waveguides placed at 0.1 mm intervals on the diaphragm were fabricated to determine the relationship between sensitivity and waveguide position. The diaphragm dimensions were (1) 2.0 mm× 10 mm× 35 μm and (2) 3.0 mm× 15 mm× 64 μm. The ratio between width and length of each diaphragm was 1:5. The maximum sensitivity of 100 mrad/kPa was obtained for the waveguide nearest to the diaphragm edge with a wavelength of 633 nm. In addition, the measured sensitivities were very similar for the corresponding waveguide positions in the two sensors since a scaling factor, which is defined as the cube of the either side length divided by the square of the thickness, was set as a constant.

Keywords: integrated optics, pressure sensor, elasto-optic effect, silicon, diaphragm

1. INTRODUCTION

Micro-opto-mechanical devices have increasingly attracted attention due to the remarkable developments in silicon micromachining technology in the past decade.[1] The integrated optic pressure sensor employing a micromachined diaphragm is one of the promising micro-opto-mechanical devices. Several groups have introduced integrated-optic interferometric pressure sensors incorporated with diaphragms since the late 1980's.[2-7] Their sensitivities are theoretically known to have a strong dependence on the position of the sensing waveguide of the phase-sensitive optical circuit[2, 8, 9], such as the Mach-Zehnder interferometer[2-4], the ring resonator[5] and the intermodal interferometer[6, 7]. According to the theoretical prediction, the sensing waveguide should be placed along the longer side of the rectangular diaphragm to maximize the sensitivity of the sensor based on the elasto-optic effect. There are, however, few reports on the experimental investigation of the sensitivity dependence with respect to the waveguide position.[6, 7] In this study, the sensitivity was experimentally examined as a function of the waveguide position in the silicon-based integrated optic pressure sensor using the intermodal interference. By using intermodal interference, many sensing waveguides, or interferometers, can be closely spaced to each other on a diaphragm, unlike the Mach-Zehnder interferometer and the ring resonator, to determine how the sensitivity is related to the waveguide position. In this experiment, two sensors were fabricated with the same scaling factor and the same side length ratio of the diaphragms. The scaling factor, which in this study is defined as the cube of the side length of the diaphragm divided by the square of the thickness, is based on the theoretical characteristics of the sensor. The two fabricated sensors allow us to verify another theoretical prediction - sensitivity does not change even if the diaphragm dimensions are changed as long as both the scaling factor and the side length ratio remain constant. As theoretically predicted, both of the sensors had almost the same sensitivities for the corresponding waveguide positions, and their maximum sensitivities were obtained at the diaphragm edge. The findings in this study are very helpful to realize the miniaturized sensor with higher sensitivity.

Electronics and Structures for MEMS II, Neil W. Bergmann, Editor,
Proceedings of SPIE Vol. 4591 (2001) © 2001 SPIE · 0277-786X/01/$15.00

2. PRINCIPLE OF SENSOR OPERATION

Fig.1 shows the integrated optic pressure sensor using intermodal interference between the fundamental TM-like and TE-like modes. The sensor has a rectangular diaphragm as a pressure-sensitive mechanical structure and a straight single-mode waveguide over the diaphragm. The diaphragm is distorted when a pressure difference is applied to the diaphragm. The distortion causes strain, which produces a change in the refractive index of the diaphragm by the elasto-optic effect. The index change yields phase retardation in the lightwave, which is propagated in the waveguide on the diaphragm. Since the phase retardation is dependent on the guided modes, the phase difference between the two modes is also a function of the applied pressure. To detect the phase difference, the sensor is placed in a pair of crossed polarizers as shown in Fig.2. The input polarizer is oriented at 45° with respect to the polarization of each guided mode. The light beam through the input polarizer is coupled to the TM-like and TE-like modes at equal intensities. At the end of the waveguide, the lightwave has linear, elliptic or circular polarization, corresponding to the induced phase difference between the two guided modes. The crossed output polarizer converts the polarization-modulated light into intensity-modulated light. The intensity of the beam passing through the output polarizer sinusoidally changes with the applied pressure. Therefore, the pressure applied to the diaphragm can be determined from the output intensity.

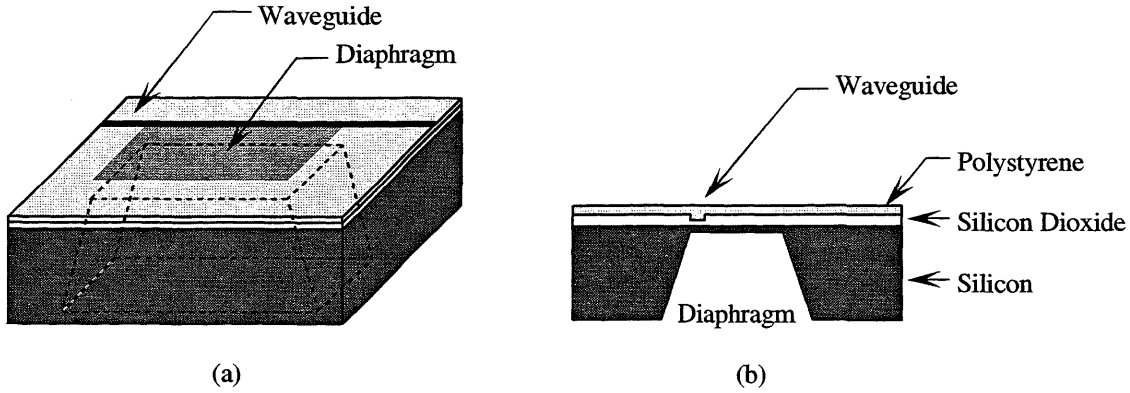

Fig. 1 (a) Schematic drawing of the integrated optic pressure sensor using intermodal interference, and (b) its cross-sectional view.

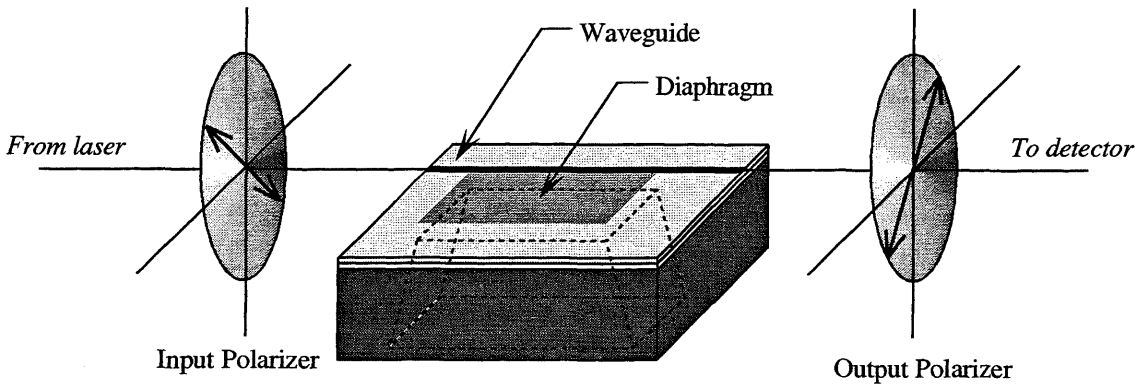

Fig. 2 A sensor system including a pair of crossed polarizers.

3. THEORETICAL SENSITIVITY VERSUS WAVEGUIDE POSITION

Since the induced anisotropic index change caused by the applied pressure is not uniformly distributed across the diaphragm, the induced phase difference is dependent on the position of the waveguide passing over the diaphragm. The phase difference per unit pressure, that is, the phase sensitivity, was calculated as a function of the waveguide position, following the mathematical description in Ref. 8. In the calculation, a rectangular diaphragm with an area of $a \times b$ and a thickness of t

was assumed. It was also assumed that the waveguide was placed parallel to side b and the pressure was uniformly applied over the diaphragm with all edges clamped. Incidentally, the theoretical calculation should be carried out using the mechanical and optical parameters of the materials which comprise the sensor. However, the parameters for polystyrene, which is the material for the guided layer of the waveguide described below, have yet to be determined. In the calculations, the parameters of fused silica were used instead of those of polystyrene. The numerical result obtained by using the parameters of fused silica would qualitatively hold true for the sensor using a polystyrene waveguide. Fig. 3 shows the calculated sensitivity versus the waveguide position. In the figure, the ratio of length and width of the diaphragm is taken as a parameter. The waveguide positions of 0 and a represent the waveguide along the edge of the diaphragm, whereas a position of $a/2$ corresponds to the center of the diaphragm. The phase sensitivities are normalized to be at unity at waveguide positions of 0 and a for each ratio. It is found that the phase sensitivities have the maximum value when the waveguide is located along the diaphragm edge, that is, at 0 and a. In other words, the diaphragm edge is the best waveguide position to maximize the sensitivity of the sensor. Moreover, the sensitivities at the edge and at the center have opposite signs, and there is a position where the sensitivity becomes zero between the edge and the center. For the diaphragm with the side length ratio of 1:5, the calculated sensitivity at the edge is about two times greater than that at the center.

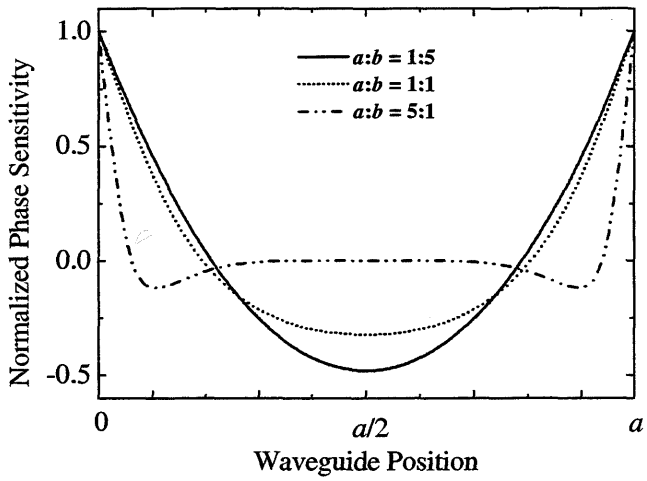

Fig. 3 Relationships between normalized phase sensitivity and waveguide position. Waveguide positions of 0 and a represent that the waveguide is placed along the edge of the diaphragm, whereas a position of $a/2$ corresponds to the center of the diaphragm.

4. EXPERIMENT

4.1. Fabrication and Measurement

Fig. 4 shows a schematic diagram of the fabricated sensors and a cross-section of the ridge-type waveguide. The sensors had straight waveguides spaced 0.1 mm apart to determine how phase sensitivity is related to waveguide position. In the fabrication, a silicon dioxide layer was first formed on both sides of the substrate by thermal oxidation. The silicon dioxide layer of the bottom surface was selectively removed by an etchant of buffered HF acid using a patterned photoresist as an etching mask. Then, the exposed silicon was anisotropically etched by KOH to produce the diaphragm. The diaphragm dimensions of two fabricated sensors were (1) 2.0 mm× 10 mm× 35 μm and (2) 3.0 mm× 15 mm× 64 μm. After diaphragm formation, the silicon dioxide was removed from the substrate and was regrown 1.0 μm in thickness, to sufficiently make the radiation loss of the guided waves into the substrate negligible. Then, shallow 10 μm wide and 0.1 μm deep grooves were formed, parallel to the diaphragm side, on the silicon dioxide layer using buffered HF acid. The polystyrene film was spin-coated as the guided layer, and its thickness at the grooves was 1.1 μm.

Fig. 5 illustrates the experimental setup to measure the output intensity versus the applied pressure. A linearly-polarized He-Ne laser at 633 nm was used in the measurement. Its polarization was set at 45° with respect to the sensor surface, so that the input polarizer shown in Fig. 2 was not necessary. The sensor was connected to a syringe by a silicone tube in order to apply pressure to the diaphragm. Pulling and pushing the plunger of the syringe caused the pressure difference, ranging from –40 kPa to 40 kPa, on the diaphragm. The positive value represents a pressure in the etched hole that is higher than that in the atmosphere.

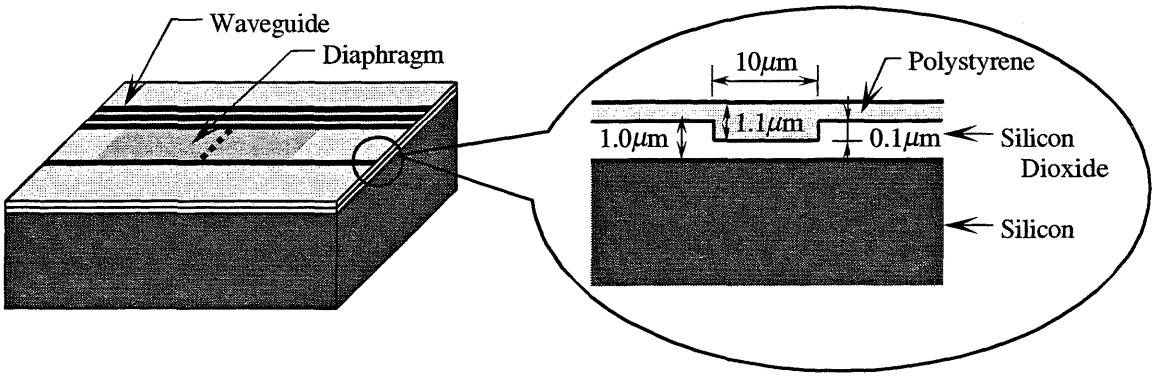

Fig. 4 Schematic drawing of the fabricated sensor and the cross-section of the waveguide. The width of the polystyrene channel waveguides was 10 μm, and the diaphragm dimensions of two fabricated sensors are (1) 2.0 mm × 10 mm× 35 μm and (2) 3.0 mm× 15 mm× 64 μm.

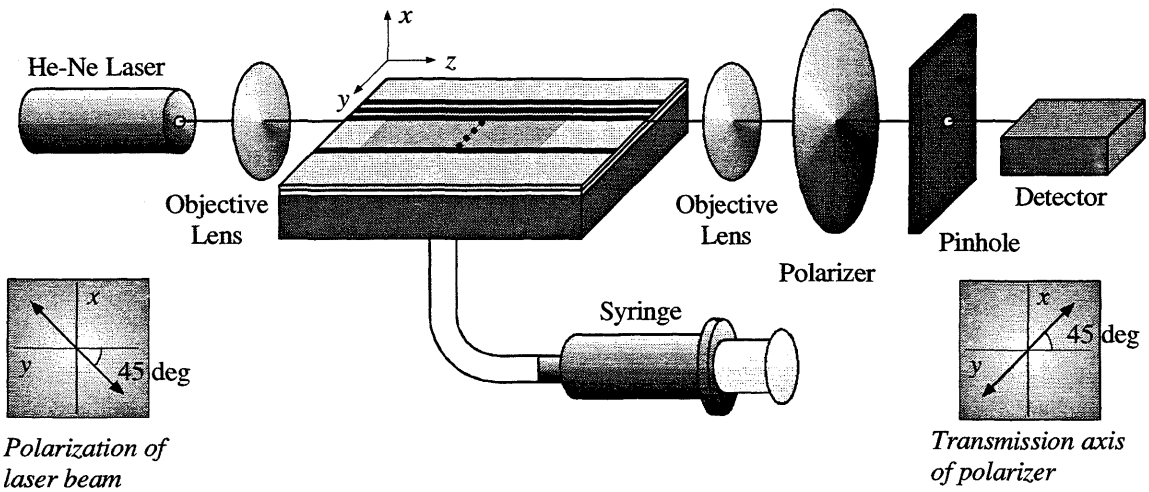

Fig. 5 The arrangement of the sensor system to measure the output intensity as a function of the applied pressure.

4.2. Experimental Results of Sensor with 2.0 mm × 10 mm × 35 μm Diaphragm

Fig. 6(a) shows the experimental result for the waveguide nearest to the diaphragm edge in the sensor with a 2.0 mm× 10 mm× 35 μm diaphragm. Also, Figs. 6(b) and (c) indicate the results for the waveguides located 0.3 mm and 1.0 mm apart from the waveguide of Fig. 6(a), respectively. The waveguide of Fig. 6(c) is the nearest to the center of the diaphragm. The solid line in each figure indicates the computer projection of the experimental data. A half period of the output intensity is called the halfwave pressure, which corresponds to the phase difference of π rad. From the obtained halfwave pressure, the phase sensitivity, defined as the resultant phase difference per unit pressure, is calculated. From Figs. 6(a) through (c), the halfwave pressures are evaluated to be 36 kPa, 1400 kPa and 44 kPa, and the corresponding phase sensitivities are 89 mrad/kPa, 2 mrad/kPa and 71 mrad/kPa, respectively. The same measurement was also taken for the other waveguide. Fig. 7 indicates the measured sensitivities for each waveguide and the theoretical curve, which reflects the calculated result in the case of $a:b=1:5$. The minus sign was added for the sensitivities near the center of the diaphragm according to the theoretical results although the sign is not distinguishable in this measurement.

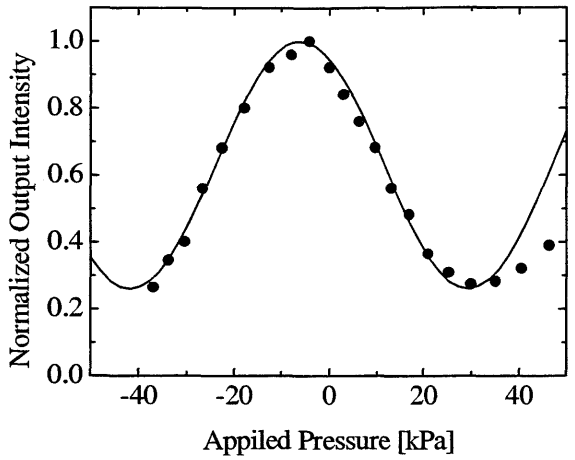

Fig. 6(a) The experimental result of normalized output intensity versus applied pressure for the waveguide nearest to the diaphragm edge.

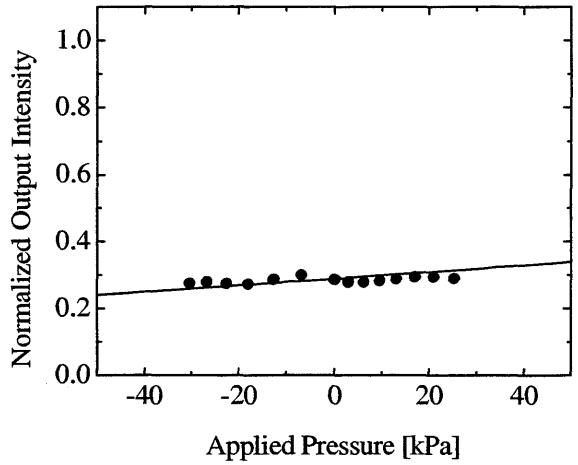

Fig. 6(b) The experimental result for the waveguide located 0.3 mm from the waveguide of Fig. 6(a).

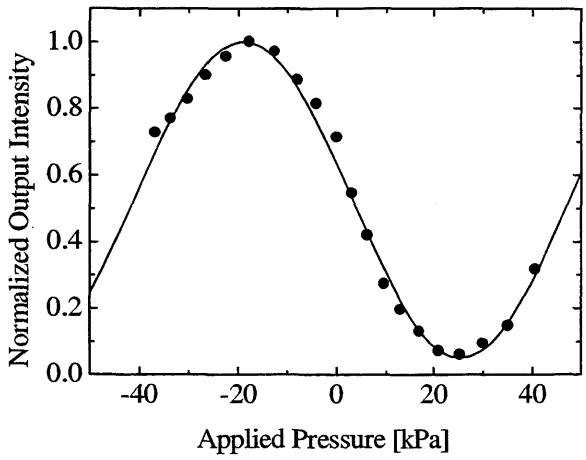

Fig. 6(c) The experimental result for the waveguide located 1.0 mm from the waveguide of Fig. 6(a). The waveguide is the nearest to the center of the diaphragm.

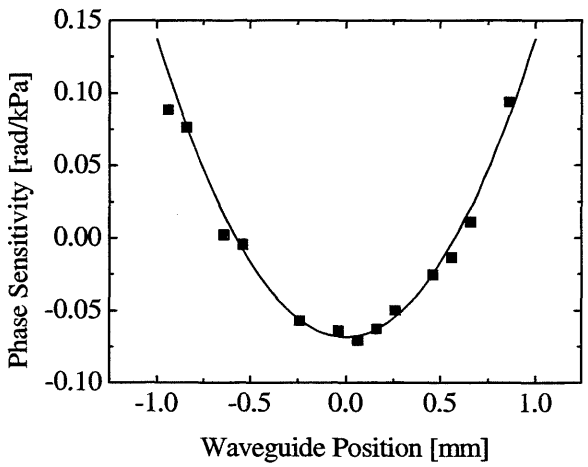

Fig. 7 Measured sensitivity as a function of the waveguide position on the diaphragm.

4.3. Experimental Results of Sensor with 3.0 mm× 15 mm× 64 μm Diaphragm

Fig. 8 shows the experimental results of the sensor with a 3.0 mm× 15 mm× 64 μm diaphragm. The waveguide position of Fig. 8(a) is the nearest to the diaphragm edge, and the waveguides of Figs. 8(b) and (c) are located 0.5 mm and 1.5 mm apart from the waveguide of Fig. 8(a), respectively. The waveguide of Fig. 8(c) is the nearest to the center of the diaphragm. From Figs. 8(a) through (c), the halfwave pressures are 31 kPa, 950 kPa and 46 kPa, and the corresponding sensitivities are 100 mrad/kPa, 3 mrad/kPa and 69 mrad/kPa, respectively. Fig. 9 shows the measured sensitivity as a function of the waveguide position and the best-fit curve, which reflects the calculated result in the case of $a:b=1:5$.

4.4. Discussions

In Figs. 7 and 9, the measured sensitivities versus the waveguide position are in good agreement with the theoretical ones although there is a slight difference near the diaphragm edge in Fig. 9. The largest sensitivity was obtained for the waveguide nearest to the edge as theoretically predicted. It is also found that sensitivity is significantly affected by a deviation of the waveguide away from the diaphragm edge.

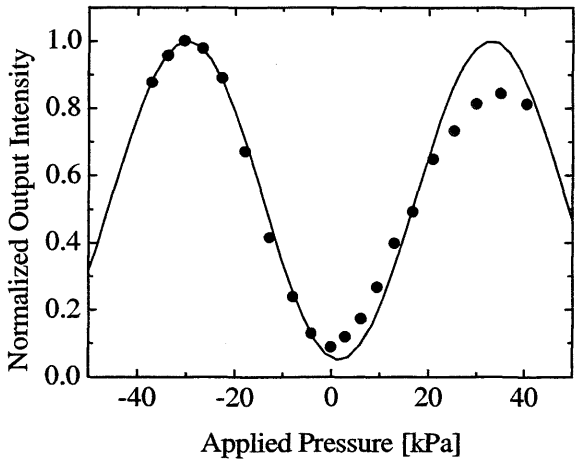

Fig. 8(a) The experimental result of normalized output intensity versus applied pressure for the waveguide nearest to the diaphragm edge.

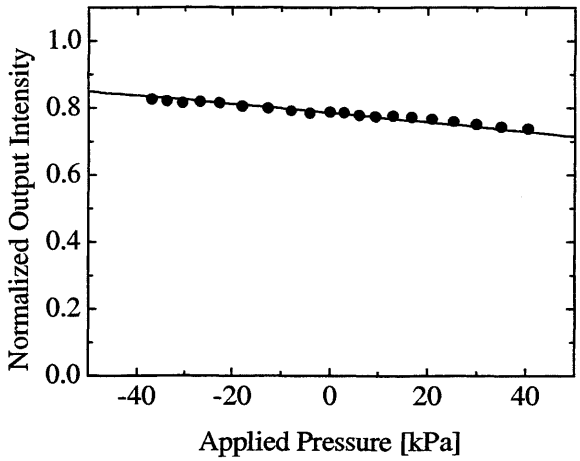

Fig. 8(b) The experimental result for the waveguide located 0.5 mm from the waveguide of Fig. 8(a).

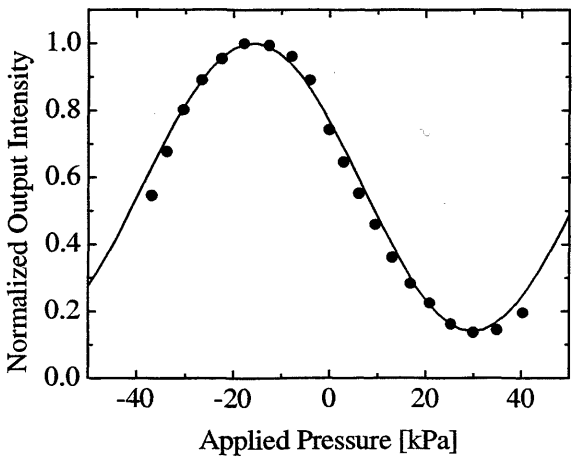

Fig. 8(c) The experimental result for the waveguide located 1.5 mm from the waveguide of Fig. 8(a). The waveguide is the nearest to the center of the diaphragm.

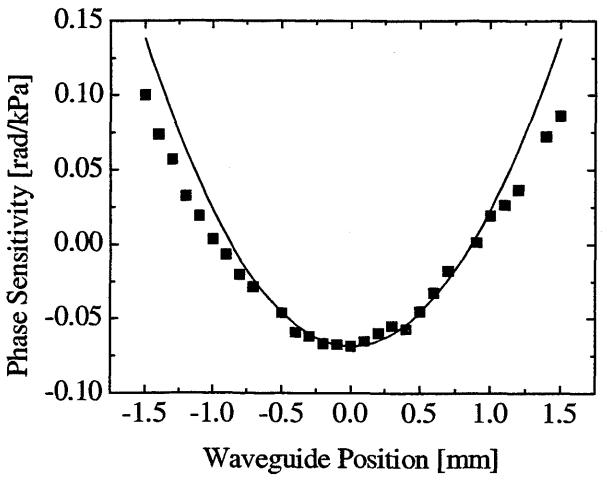

Fig. 9 Measured sensitivity as a function of the waveguide position on the diaphragm.

Incidentally, sensitivity is theoretically known to be proportional to the cube of the either side length of the diaphragm if the thickness t and the side length ratio a/b remain unchanged.[8,9] It is also inversely proportional to the square of the thickness of the diaphragm when the width a and the length b are kept constant.[8] Therefore, in any diaphragms with the same side length ratio a/b, the sensitivity does not change as long as the scaling factor a^3/t^2 remains constant. The fabricated sensors have the same scaling factor and the same side length ratio. Table 1 shows the sensitivities of the fabricated sensors for the waveguides nearest to the edge and nearest to the center. The sensitivities of the sensors are very similar to each other as theoretically predicted. In comparison, the measured sensitivities for the waveguides nearest to the center are 70% to 80% of those nearest to the edge although the theoretical percentage is about 50%. The difference was caused by the following facts. We did not, unfortunately, have any waveguides just on the edge, where the sensitivity rapidly decreases as the waveguide deviates from the edge. So the measured sensitivity near the edge did not attain the expected value at the edge. In contrast, the small deviation of the waveguide from the center did not affect the sensitivity very much. In addition, the waveguides of the fabricated sensors were not completely parallel to the side of the diaphragm.

Moreover, it is found from Figs. 6 and 8 that the extinction ratios are about 10dB, and initial phase differences exist between the guided modes. The low extinction ratios were attributed to stray light through the pinhole. The non-zero initial phase differences arose from the difference between the effective indices of the guided modes. If the effective index difference is relatively large, the initial phase difference can be adjusted by changing the waveguide length.

Table 1 Diaphragm dimensions, side length ratios, scaling factors and measured sensitivities of the fabricated sensors

		SENSOR #1	SENSOR #2
Diaphragm dimensions	Width a [mm]	2.0	3.0
	Length b [mm]	10	15
	Thickness t [μm]	35	64
Ratio between length and width $a:b$		1 : 5	1 : 5
Scaling factor a^3/t^2		6.5×10^3	6.6×10^3
Sensitivity for waveguide nearest to edge [mrad/kPa]		89	100
Sensitivity for waveguide nearest to center [mrad/kPa]		–71	–69

5. CONCLUSIONS

We experimentally examined the relationship between sensitivity and waveguide position in the silicon-based integrated optic pressure sensor with a micromachined diaphragm. It was found that the diaphragm edge is the best position to maximize the sensitivity of the sensor. In addition, it was experimentally proved that the sensitivity does not change even if the diaphragm dimensions are changed as long as the ratio a/b and the scaling factor a^3/t^2 remain constant. Incidentally, one of the targets of our studies is to develop an integrated optic pressure sensor to be incorporated into a catheter for blood pressure measurement. The largest sensitivity of 100 mrad/kPa obtained in this study is sufficient for blood pressure measurement although the sensor must be further miniaturized. The sensor can be miniaturized with no change in sensitivity if the diaphragm is made smaller and thinner while both the ratio a/b and the scaling factor a^3/t^2 are kept constant.

ACKNOWLEDGEMENT

This work is, in part, supported by a Grant-in-Aid for Scientific Research (No.12650339) from the Japan Society for the Promotion of Science.

REFERENCES

1. M. Tabib-Azar, and G. Beheim, "Modern trends in microstructures and integrated optics for communication, sensing, and actuation," Opt. Eng., **36**, pp.1307-1318, 1997.
2. M. Ohkawa, M. Izutsu, and T. Sueta, "Integrated optic pressure sensor on silicon substrate," Appl. Opt., **28**, pp.5153-5157, 1989.
3. G. N. De Brabander, Glenn Beheim, and J. T. Boyd, "Integrated optical micromachined pressure sensor with spectrally encoded output and temperature compensation," Appl. Opt., **37**, pp.3264-3267, 1998.
4. H. Porte, V. Gorel, S. Kiryenko, J. Goedgebuer, W. Daniau, and P. Blind, "Imbalanced Mach-Zehnder interferometer integrated in micromachined silicon substrate for pressure sensor," J. Lightwave Technol., **17**, pp.229-233, 1999.
5. G. N. De Brabander, J. T. Boyd, and G. Beheim, "Integrated optical ring resonator with micromechanical diaphragm for pressure sensing," IEEE Photon. Technol. Lett., **6**, pp.671-673, 1994.
6. Y. Shirai, T. Goto, M. Ohkawa, S. Sekine, and T. Sato, "Silicon-based integrated optical pressure sensor using intermodal interference between TM-like and TE-like modes," Proc. SPIE, 4277, pp.411-418, 2001.
7. A. Yamada, Y. Shirai, T. Goto, M. Ohkawa, S. Sekine, and T. Sato, "Relationship between sensitivity and waveguide position on diaphragm for silicon-based integrated optic pressure sensor," in *Technical Digest Volume-I, CLEO/Pacific Rim 2001*, pp.420-421, 2001.
8. M. Ohkawa, T. Abe, S. Sekine, and T. Sato, "Integrated optic micropressure sensor using ring resonator," Electronics and Communications in Japan, **79**, pp.1-10, 1996.
9. M. Ohkawa, K. Hasebe, C. Nishiwaki, S. Sekine, and T. Sato, "Integrated optical pressure sensor using intermodal interference between two mutual orthogonal guided-modes," Optical Review, **7**, pp.144-148, 2000.

* Correspondence: E-mail: ohkawa@eng.niigata-u.ac.jp; Telephone & Fax: +81-25-262-6734